1

Development Optimization of Horizontal Wellbores Using Lamé Elastic Constants from 3D Seismic

Dr. Michael Shoemaker*, Santhosh Narasimhan(1), Josh Peacock, John Becher, Jake Lacy, Brittney Ferguson, Nancy Zakhour,
Chesney Petkovsek, Callon Petroleum Company, Houston Texas (1) Premier Oilfield Group, Houston Texas

Introduction

Technological advancements in horizontal drilling and fracture stimulation of tight oil formations have resulted in the resurgence of the century-old mature Permian Basin (Figure 1a). Current development strategies typically involve a "harvesting" approach whereby multi-well pads are used to drill stacked horizontal layers within the Spraberry and Wolfcamp formations (Figure 1b) in a repeated sequence, implementing identical geometric stage placement. As such, these methods assume similar rock properties and in-situ stress states along horizontal wellbores which can be problematic. This can result in undesirable effects such as well underperformance, pressure sinks from nearby depletion,

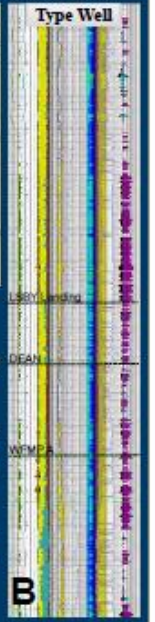

Figure 1. A) Permian Basin locator and B) type well with landing point

and well-bashing resulting from unintentional stimulation and communication of nearby producing wells. In hopes of mitigating such quandaries, more operators are increasingly implementing development strategies that encompass evolving subsurface technology and workflows that integrate multi-domain data types including geology and stratigraphy, petrophysics (Figure 2), and rock physics (Figure 3) integrated with geomechanics (Figure 4) and 3D seismic (Figure 5) for stress estimates used for fracture geometry modeling calibrated to microseismic data, reservoir engineering parameters, and production history matching. Stress profiles, both vertically and along horizontal wellbores, can now be extrapolated from a final 3D mechanical earth model representing in-situ minimum horizontal stress that has been calibrated to core to account for local anisotropy effects.

Figure 2. Petrophysics classification: lithofacies 1 and 2 define reservoir quality characteristic of higher minimum horizontal stress while 3 and 4 define completion quality and landing zones characteristic of relatively lower minimum horizontal stress.

Objective

We propose a new method to estimate minimum horizontal stress vertically and along lateral wellbores in 3D space. The method integrates multi-domain data sets with Lamé elastic constants from 3D seismic which provides the necessary heterogeneity of in-situ stress states to effectively model fracture geometries for frac optimization and horizontal landing.

Method

This method presents an empirical approach based on the integration of said multi-domain data types calibrated to AVO reflection seismic data inverted for compressional wave velocity (Vp), and shear wave velocity (Vs), but expressed in equal terms of Lamé elastic constants defined by lambda (λ) or incompressibility, and mu (μ) for rigidity and is equivalent to shear modulus. For geomechanics, Lambda and mu define Hooke's law relating stress to strain which intrinsically defines the fracability of "brittle" (low stress) rocks and ductile (high stress) rocks. Subsequently, Goodway (2010) shows that Lambda and Mu define the isotropic Closure Stress Scalar (CSS) defined as:

$$CSS_{ISO} = \frac{\lambda}{\lambda+2\mu} = \frac{\upsilon}{(1-\upsilon)}, \qquad (1)$$

which is equivalent to the Bound Poisson's Ratio (υ). This expression represents a rock quality term embedded within the isotropic Uniaxial Strain Equation defined as:

$$S_h = \frac{\upsilon}{(1-\upsilon)}\left(S_v - \alpha P_p\right) + P_p + Tectonic, \qquad (2)$$

where S_h equals the minimum horizontal stress required to fracture the rock given overburden stress (S_v), Biot's constant (α), and pore pressure of the formation (P_p).

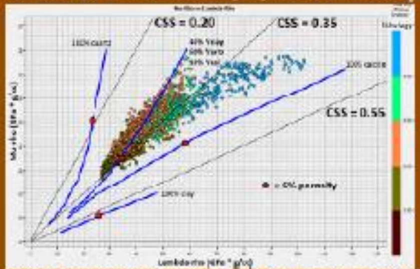

Figure 3. Rock physics template of lambda-mu-rho (LMR) with closure stress scalars and lithofacies classification defined in Figure 2. Data points were taken from the Top Lower Spraberry to Wolfcamp C.

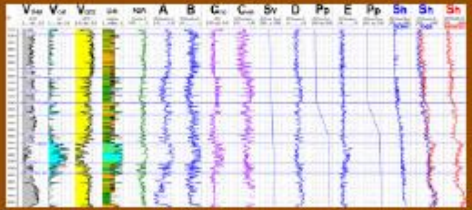

Figure 4. 1D Mechanical earth Model (MEM) showing the seven terms defined in Equation 5. Minimum horizontal stress (S_h) profiles represent the log / core based solution (blue curve) and seismic based solution (red curve) using the seismic Closure Stress Scalar corrected for anisotropy.

A B C S_v D P_p E P_p

$$S_h = \left(\frac{E_{sh}}{E_{sv}}\right) * C\frac{\lambda}{\lambda+2\mu}\left(S_v - \alpha_v P_p\right) + \left(\alpha_h P_p\right) + Tectonic$$

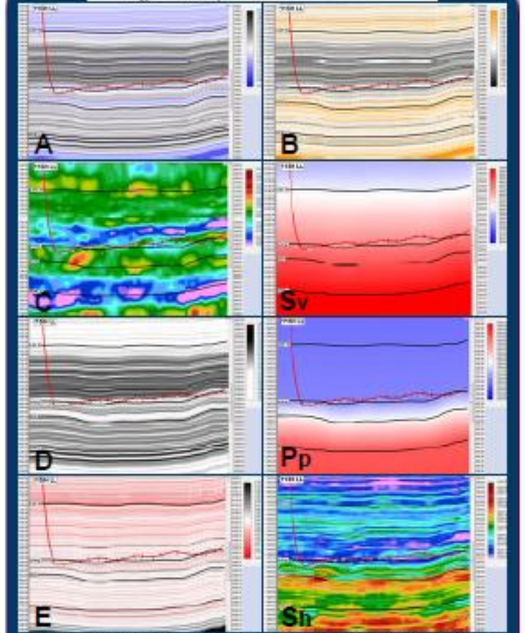

Figure 5. Cross sections from 3D cubes (resampled at 1ft) representing the mechanical terms defined in Equation 5 which are: A) $\left(\frac{E_{sh}}{E_{sv}}\right)$ the modulus of anisotropy, B) C is the anisotropic Bound Poisson's Ratio Scalar, C) $\frac{\lambda}{\lambda+2\mu}$ is the isotropic Closure Stress Scalar from seismic, S_v) overburden stress, D) α_v is Biot's constant in the vertical direction, Pp) pore pressure, E) α_h is Biot's constant in the horizontal direction, Sh) resulting minimum horizontal stress showing vertical and horizontal stress heterogeneity. Panel letters also define terms defined in Equation 5.

Figure 3 is a rock physics template that shows multi-domain relationships between geomechanical properties Lambda-Mu-Rho (LMR) with respect to changes in CSS, lithofacies (Figure 2), and porosity. Lower CSS typically results in optimal landing zones.

Local anisotropy effects were investigated and measured using compressional sonic and shear logs calibrated to triaxial core data from the area. Narasimhan (2016) provides a valid workflow implementing a Ben Eaton anisotropic stress model for converting static mechanical measurements from core to dynamic velocity measurements. Resulting anisotropic scalars, representing correction factors to isotropic terms from Equation 2, are defined in Equation 3:

$$S_h = \left(\frac{E_{sh}}{E_{sv}}\right)\frac{\upsilon_{sv}}{(1-\upsilon_{sh})}\left(S_v - \alpha_v P_p\right) + \left(\alpha_h P_p\right) + Tectonic, \qquad (3)$$

where $\frac{E_{sh}}{E_{sv}}$ is the anisotropic modulus and $\frac{\upsilon_{sv}}{(1-\upsilon_{sh})}$ is the anisotropic BPR.

Magnitude of the differential between the anisotropic and isotropic Bound Poisson's Ratio (BPR) can be calculated to represent an anisotropic correction scalar that's applied to the isotropic Closure Stress Scalar (CSS) defined in Equation 1 represented by:

$$CSS_{ANI} = C\frac{\lambda}{\lambda+2\mu} = \frac{\upsilon_{sv}}{(1-\upsilon_{sh})}, \qquad (4)$$

where C is the anisotropic BPR scalar which equals the isotropic BPR less any anisotropic effects ($C = 1$). Equation 4 can now be inserted into Equation 3, and minimum horizontal stress calculated using anisotropic corrected mechanical properties defined by the AVO inverted seismic CSS where:

$$S_h = \left(\frac{E_{sh}}{E_{sv}}\right) * C\frac{\lambda}{\lambda+2\mu}\left(S_v - \alpha_v P_p\right) + \left(\alpha_h P_p\right) + Tectonic. \qquad (5)$$

Figure 4 shows each of the terms from Equation 5 in log form and resampled equally at 1 ft, with formation tops including the Lower Spraberry and Wolfcamp, and defines the 1D Mechanical Earth Model (MEM) relating mineralogy and lithofacies to rock mechanics, and defines effective stress and pore pressure gradients. The geomechanical terms / curves were interpolated away from the 1D MEM location (Figures 7 and 8) to areas of interest using the seismic framework horizons and existing vertical wells as constraints to preserve formation thickness. This results in seven 3D geomechanical cubes sampled equally at 1ft including the 3D seismic CSS term. Figure 5 shows identical cross sections for all terms along a Lower Spraberry lateral wellbore (11SH LL) near the 1D MEM location shown in Figure 7, which also defines the areal extent of the 3D cubes. The lower right panel (Figure 5) shows the cross section representing the final 3D (S_h) minimum horizontal stress cube defined at a 1 ft vertical and horizontal sample rate.

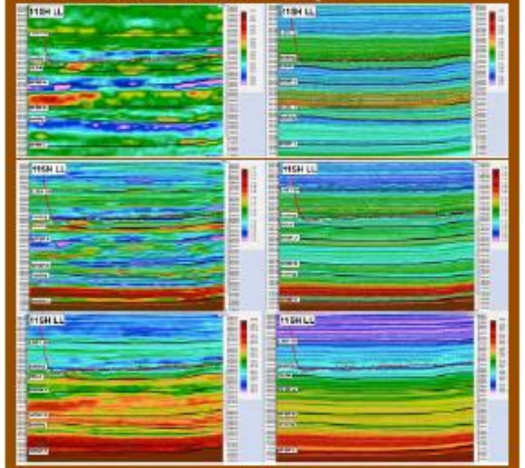

Figure 6. Comparison of calculated minimum horizontal stress using isotropic vs. anisotropic Closure Stress Scalar data without stress gradient. The top panel shows CSS calculated using isotropic seismic (left) and isotropic CSS from logs (right). The middle panel shows the same data corrected for anisotropy using correction scalars. The bottom panel shows the final minimum horizontal stress solution (Sh) corrected for anisotropy using CSS from seismic (bottom-left) and logs (bottom-right).

Development Optimization of Horizontal Wellbores Using Lamé Elastic Constants from 3D Seismic

Dr. Michael Shoemaker*, Santhosh Narasimhan(1), Josh Peacock, John Becher, Jake Lacy, Brittney Ferguson, Nancy Zakhour,
Chesney Petkovsek, Callon Petroleum Company, Houston Texas (1) Premier Oilfield Group, Houston Texas

Results

A 3D stress cube, calculated using Equation 5 with Lamé elastic constants from 3D seismic, has successfully characterized reservoir and completion quality within the Spraberry and Wolfcamp formations. Lambda-rho and Mu-rho (LMR) cross plots, calibrated to lithofacies, geomechanics, and rock physics templates, were used to guide in-situ stress state interpretation in identifying stress heterogeneity for acreage development strategies and along horizontal wellbores for completion optimization.

Other seismic methods are isotropic, and become less effective and measure stress errors in formations that are significantly anisotropic (e.g., source rocks) due to laminations, etc. Figure 6 shows the isotropic Closure Stress Scalar calculated using seismic and from logs before and after the anisotropy correction (scalars) were applied. Particularly, isotropic CSS calculated from both seismic and logs (Figure 6, top panels) show anomalously low

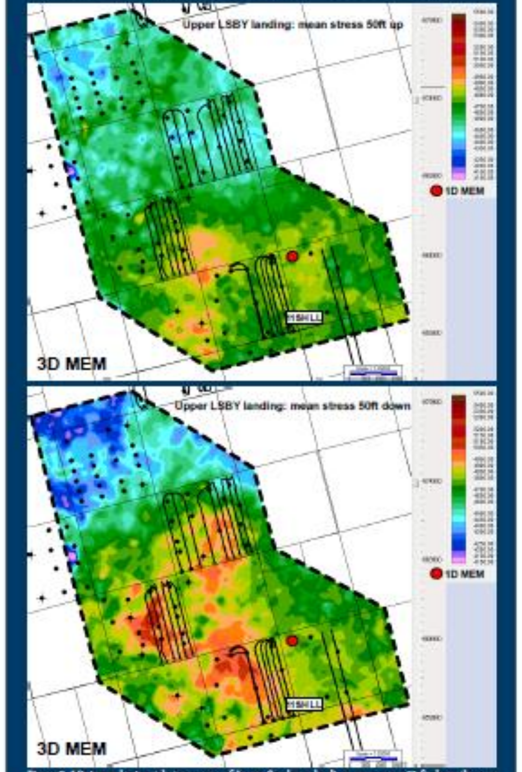

Figure 7. Minimum horizontal stress maps of Lower Spraberry landing zone, mean 50 ft above the zone (top panel) and 50 ft below (bottom panel). The red dot locates the 1D MEM. Areas showing relatively higher minimum stress (red) would likely be more resistive to pressure sinks from depletion.

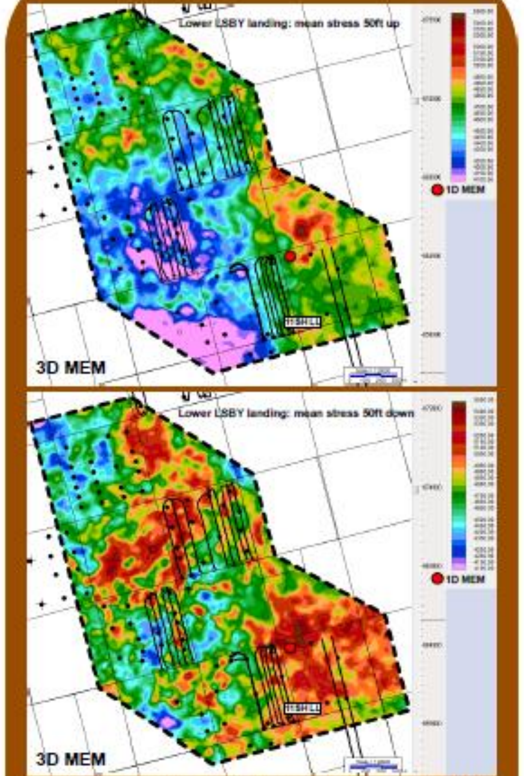

Figure 8. Minimum horizontal stress maps of Upper lower Spraberry landing zone, mean 50 ft above the landing zone (top panel) and 50 ft below (bottom panel). The red dot locates the 1D MEM. Areas showing relatively lower minimum stress (blue/purple) would likely be more prone to pressure sinks from depleting parent wells.

stress at flooding surfaces (e.g., WFMP A, B and C) represent organically rich reservoir rocks (lithofacies 1 and 2) that are anisotropic (Figure 5, terms A and B). Increased stress values result after anisotropy corrections are applied (middle and bottom panels). For completion quality, ideal landing zones typically require less anisotropy correction, or when the anisotropic Bound Poison's Ratio scalar (term C) is equal to or slightly less then one, and is characteristic of increased volume of calcite and quartz (Figure 2, lithofacies 3 and 4). However, organically rich (source) rocks for reservoir quality typically require significantly higher anisotropic corrections due to increased organics and clay, and have higher stresses and are ductile. This is observed in Figure 6. The landing zone for the Lower SPRB and WFMP A (Figure 6) show relatively minimal stress changes before and after anisotropy corrections are applied, and hence are relatively more isotropic.

Figures 7 and 8 show minimum horizontal stress maps of the Lower and Upper Lower Spraberry landing zones, respectively. Development strategies can now be optimized regionally, governed by stress variability. Generally, blue highlighted areas, characteristic of relatively lower stress (more brittle), may be at greater risk for pressure sinks from "parent" well depletion. Alternatively, yellow/red colors show areas of higher stress that may be conducive to increased fracture containment horizontally and vertically, potentially resulting in less frac-bashing, examples which are also seen in cross section (Figure 9) showing the added stress variability from seismic.. For completion optimization, the 3D stress cube sampled at 1 ft now allows for the extrapolation of vertical stress profiles (Figure 10, black curves) at anomalous segments along horizontal wellbores for fracture geometry modeling when testing treatment sensitivities and parameterization. Figure 11 shows a horizontal stress profile correlated to shear modulus (or mu) as well as the

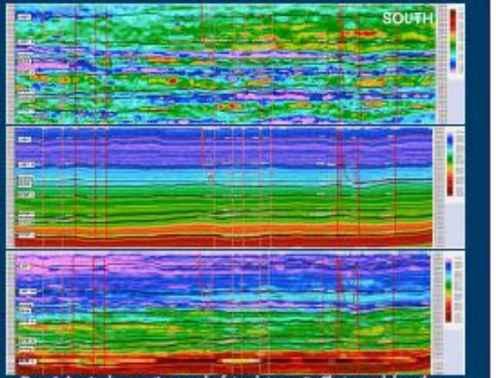

Figure 9. A regional cross section example of stress heterogeneity. The top panel shows the isotropic CSS, middle panel shows minimum horizontal stress using CSS from logs (Equation 3) , and a final stress solution (bottom panel) integrating the anisotropic CSS from seismic (Equation 5).

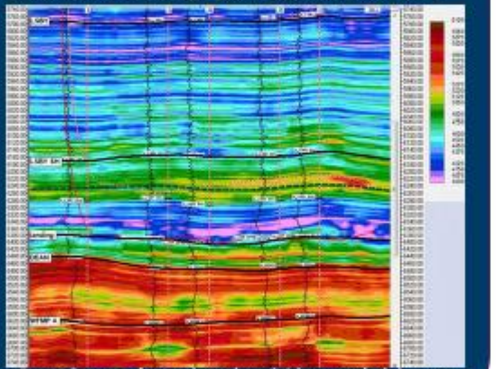

Figure 10. Cross section of minimum horizontal stress that's been integrated with closure stress scalar (CSS) from seismic data. Black curves represent stress profiles used to model fracture geometry.

anisotropic corrected CSS from the seismic and rate of penetration (ROP) from drilling data which show good correlations. This example shows the high magnitude of stress variability lengthwise and vertically along the lateral, which can now be fracture modeled for a more optimal treatment design on a stage-by-stage basis and for optimal landing.

Conclusions

The method successfully integrated multi-domain data sets with Lamé elastic constants from 3D seismic, and provided the necessary heterogeneity of in-situ stress states to effectively model fracture geometries for frac optimization and horizontal landing, both vertically and horizontally in 3D space. Examples of fracture modeling is shown in

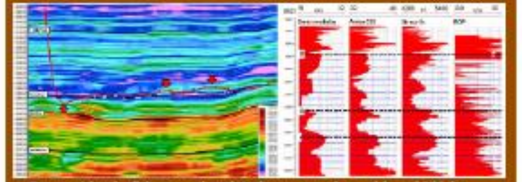

Figure 11. A lateral well showing good correlation between stress, shear modulus, and ROP data.

Figure 12 that simulates fracture geometry and propagation (Cherian et al., 2015) which ultimately match fracture treating pressures measured in the field, shown in Figure 13. Undesirable effects related to parent-child well relationships such as production underperformance, less effective asymmetrical stimulation, or well-bashing can now be investigated at greater detail using stress heterogeneities provided by this method.

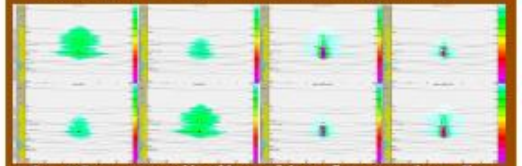

Figure 12. Fracture geometry modeling of the type-well showing effective proppant placement. Planar fractures occur in areas of less stress, while complex fractures typically occur in areas of high stress.

Figure 13. Treatment plot measured in the field that is pressure history matched when fracture modeling.

Literature Cited

Cherian, B. V., McClary, M., Fluckiger, S., Nieuwdorp, N., Bandy, B., Edwards, S., ... Shaikh, H. (2015, October 20). Production Performance in the In-Fill Development of Unconventional Resources. Society of Petroleum Engineers.

Goodway, B., M. Perez, J. Varsek, and C. Abaco, 2010, Seismic petrophysics and isotropic-anisotropic AVO methods for unconventional gas exploration: *The Leading Edge*, 29, no. 12, 1500–1508.

Narasimhan, S., Shaikh, H., Gray, J. K., Cherian, B. V., Olaoye, O., Rifai, R., ... Sharf-Aldin, M. (2016, February 1). Effect of Horizontal Stress Models and Biot Poro-Elasticity on Predicted Fracture Geometry. Society of Petroleum Engineers. doi:10.2118/179162-MS